INTERNATIONAL JOURNAL OF NUMERICAL MODELLING: ELECTRONIC NETWORKS, DEVICES AND FIELDS
Int. J. Numer. Model. 0000; **00**:1–9
Published online in Wiley InterScience (www.interscience.wiley.com). DOI: 10.1002/jnm

Analysis of transient scattering problems using a discontinuous Galerkin method: application to the shielding effectiveness of enclosures with heterogeneous walls

M. Boubekeur[1], A. Kameni[1], L. Pichon[1], A. Modave[2], C. Geuzaine[2]

[1] *Laboratoire de Génie Electrique de Paris, 11 rue Joliot-Curie, 91192 Gif-sur-Yvette, France*
[2] *Université de Liège, Department of Electrical Engineering and Computer Science, Montefiore Institute, Belgique*

SUMMARY

In this paper, different formulations of Maxwell equations are combined for computing the shielding effectiveness of enclosures made from heterogeneous periodic materials. The validity of the homogenized parameters given by Maxwell-Garnett rules in the frequency domain are tested in the time domain using a nodal discontinuous Galerkin method, which uses an interface condition based on analytical solution in the frequency domain to replace a conductive sheet. This interface condition allows to avoid meshing the thin sheet, thus reducing the computational cost. Results of scattering by composite enclosures are presented in the frequency domain thanks to a Fast Fourier Transform.

Received ...

KEY WORDS: Discontinuous Galerkin Method, Maxwell's equations, time domain, frequency domain, homogenization, shielding effectiveness

1. INTRODUCTION

The diversification of materials in advanced technological industries has increased the complexity of the problems linked to the coexistence of systems. This is particularly the case for embedded systems, which are increasingly manufactured from heterogeneous composite materials. The study of electromagnetic compatibility problems when such materials are used can be realized through homogenization techniques and efficient numerical methods [1][2]. It becomes useful to introduce strategies that combine different modeling approaches to compute characteristics such as shielding effectiveness.

In this article we propose a process based on solving the Maxwell's equations in the time domain using a nodal discontinuous Galerkin method in the time domain in order to evaluate the shielding effectiveness of enclosures. The result is compared to a result obtained with Method of Moments (MoM) in the frequency domain [3][4]. This method takes account the transient regime and a large band of frequency can be excited in one simulation. In the frequency domain, the transient regime is neglected. For enclosures made from heterogeneous periodic materials [5][6]. This work combines the numerical analysis of homogenization rules [7][8] and an interface condition based on analytical solution in the frequency domain in homogeneous media. This interface condition is proposed to avoid meshing the thin conductive sheet, thus reducing the computational cost. The shielding effectiveness in the frequency domain is computed by considering transient gaussian pulses as incident fields. The results are obtained from the Fourier transform of both incident and transmitted fields.

2. ENCLOSURE MODELING

2.1. Discontinuous Galerkin method

Consider the time-evolution of the electric field E, the electric induction D, the magnetic field H, the magnetic induction B and the current density J. In this work, physical media are assumed to be homogeneous and linear. These fields are connected by the constitutive relations

$$B = \mu H, \quad D = \epsilon E \quad \text{and} \quad J = \sigma E, \tag{1}$$

where $\epsilon = \epsilon(x)$ is the permittivity of the medium, $\mu = \mu(x)$ is its permeability and $\sigma = \sigma(x)$ is its conductivity. Therefore, Maxwell's equations can be reduced to the system

$$\begin{cases} \epsilon \partial_t E - \nabla \times H = -\sigma E, \\ \mu \partial_t H + \nabla \times E = 0, \end{cases} \tag{2}$$

where only E and H are considered as unknowns.

The discontinuous Galerkin method was introduced for solving the conservative form of partial differential equations [9]. This method consists in discretizing the variational formulation of (2) on each mesh element T of the domain $\Omega = \cup T$,

$$\begin{cases} \displaystyle\int_T \epsilon \partial_t E \phi - \int_T H \times \nabla \phi - \int_{\partial T} (n \times H)^{\text{num}} \phi = - \int_T \sigma E \phi, \\ \displaystyle\int_T \mu \partial_t H \psi + \int_T E \times \nabla \psi + \int_{\partial T} (n \times E)^{\text{num}} \psi = 0, \end{cases} \tag{3}$$

where ϕ and ψ are test functions. Numerical values of $(n \times H)^{\text{num}}$ and $(n \times E)^{\text{num}}$ are defined in the interface terms to connect adjacent elements . Different formulations of the numerical fluxes exist [6] [10] [11]. The following expressions resulting in different numerical schemes are implemented:

$$\begin{cases} (n \times H)^{\text{num}} = n \times \dfrac{\{ZH\}}{\{Z\}} - \alpha \left(n \times \dfrac{(n \times [E])}{\{Z\}} \right), \\ (n \times E)^{\text{num}} = n \times \dfrac{\{YE\}}{\{Y\}} + \alpha \left(n \times \dfrac{(n \times [H])}{\{Y\}} \right), \end{cases} \tag{4}$$

where $Z = \sqrt{\mu/\epsilon}$ is the impedance of the medium and $Y = \sqrt{\epsilon/\mu}$ is its admittance. For $\alpha = 0$, centred fluxes are obtained and the numerical scheme is dispersive[12]. For $\alpha = 1$, upwind fluxes are obtained and the numerical scheme is dissipative[6]. The notations $[\cdot]$ and $\{\cdot\}$ are used for the jump and the mean value of a quantity at the interface, *i.e.*

$$[u] = \frac{u^+ - u^-}{2} \quad \text{and} \quad \{u\} = \frac{u^+ + u^-}{2}, \tag{5}$$

where the subscript '$-$' denotes the value of the quantity u in the current element, while '$+$' is for the adjacent element.

2.2. An interface condition for thin conducting sheets

In order to design the new interface condition, consider the transverse electric one-dimensional case of time-harmonic Maxwell's equations in the sheet:

$$\begin{cases} \partial_x E = \jmath \omega \mu H, \\ \partial_x H = -(\sigma + \jmath \omega \epsilon) E, \end{cases} \tag{6}$$

where ϵ, μ and σ are constants (Figure 1). Using the analytical 1D solution, the electromagnetic fields on both sides of the sheet are connected by:

$$\begin{pmatrix} E(\omega, d) \\ H(\omega, d) \end{pmatrix} = \begin{pmatrix} \cosh(\gamma d) & \eta \sinh(\gamma d) \\ \frac{1}{\eta} \sinh(\gamma d) & \cosh(\gamma d) \end{pmatrix} \begin{pmatrix} E(\omega, 0) \\ H(\omega, 0) \end{pmatrix}, \tag{7}$$

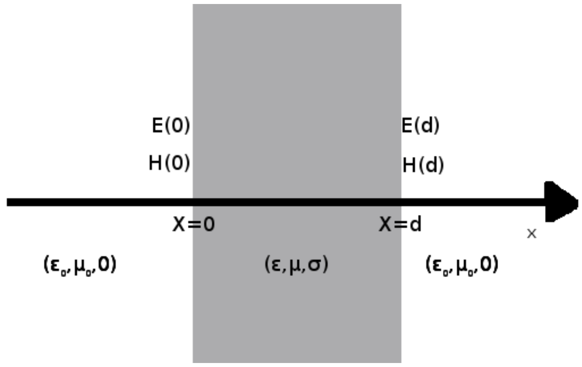

Figure 1. Geometry of the problem with the thin conducting sheet.

where η is the intrinsic impedance of the sheet:

$$\eta = \sqrt{\frac{\jmath\omega\mu}{\sigma + \jmath\omega\epsilon}}, \tag{8}$$

and γ the planar propagation constant:

$$\gamma = \sqrt{\jmath\omega\mu(\sigma + \jmath\omega\epsilon)}. \tag{9}$$

At low frequencies, $\jmath\omega\epsilon$ can be neglected. The impedance and the propagation constant can be approximated by:

$$\eta \approx \sqrt{\frac{\jmath\omega\mu}{\sigma}} \quad \text{and} \quad \gamma \approx \sqrt{\jmath\omega\mu\sigma}, \tag{10}$$

and the relation (7) can be rewritten as an admittance relation for a layer:

$$\begin{pmatrix} H(\omega,0) \\ H(\omega,d) \end{pmatrix} = \begin{pmatrix} y_1(\omega) & -y_2(\omega) \\ y_2(\omega) & -y_1(\omega) \end{pmatrix} \begin{pmatrix} E(\omega,0) \\ E(\omega,d) \end{pmatrix}, \tag{11}$$

with

$$\begin{cases} y_1 = -\dfrac{1}{\eta}\dfrac{1}{\tanh(\gamma d)}, \\ y_2 = -\dfrac{1}{\eta}\dfrac{1}{\sinh(\gamma d)}. \end{cases} \tag{12}$$

When $\omega \longrightarrow 0$, the asymptotic behaviour of y_1 and y_2 is

$$\begin{cases} y_1 = -\dfrac{\jmath}{\omega\mu d} - \dfrac{\sigma d}{3} + \Theta(\omega), \\ y_2 = -\dfrac{\jmath}{\omega\mu d} + \dfrac{\sigma d}{6} + \Theta(\omega). \end{cases} \tag{13}$$

Assuming the continuity of the electric field E, and using the relation (11) with (13) for H, simplified relations between the fields of both sides of the sheet are obtained:

$$\begin{cases} E(\omega,d) = E(\omega,0), \\ H(\omega,d) - H(\omega,0) = \sigma d \dfrac{E(\omega,0) + E(\omega,d)}{2}. \end{cases} \tag{14}$$

This approach neglects the skin depth. So,this relation is valid if d is smaller than the skin depth δ, *i.e.*

$$d \ < \ \delta = \sqrt{\frac{2}{\omega\mu\sigma}}. \tag{15}$$

DOI: 10.1002/jnm

For the time domain application, the previous relation in the frequency domain can be written:

$$\begin{cases} E(t,d) = E(t,0), \\ H(t,d) - H(t,0) = Y_s \dfrac{E(t,0)+E(t,d)}{2}. \end{cases} \tag{16}$$

where $Y_s = \sigma d$. This relation can be formulated with the tangential components of the fields:

$$\begin{cases} n \times E(t,d) = n \times E(t,0) \\ n \times H(t,d) - n \times H(t,0) = Y_s\, n \times \left(n \times \dfrac{E(t,0)+E(t,d)}{2} \right) \end{cases} \tag{17}$$

where n is the outward normal of the element corresponding to'$-$'. Note that this description is also valid for the transverse electric case and is implemented in $2D$ and $3D$.

2.3. Implementation of the interface condition in the DG scheme

A specific interface term must be developed to consider the interface condition (17) in the DG scheme. The aim is to use a geometry with the interface illustrated in Figure 2(a), instead of the real geometry with the sheet shown in Figure 2(b).

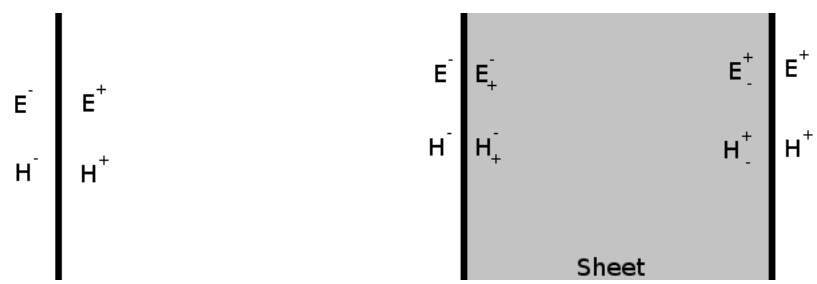

(a) used geometry (b) real geometry

Figure 2. Geometry of the problem with the interface condition (a) or the sheet (b).

To calculate the interface term for the current element (with '$-$'), we assume:

- the continuity of the tangential components of the electric field in the sheet, *i.e.*

$$n \times E^- = n \times E^-_+ = n \times E^+_- = n \times E^+, \tag{18}$$

- the continuity of the tangential components of the magnetic field at the interface between the sheet medium and the air, *i.e.*

$$\begin{cases} n \times H^- = n \times H^-_+, \\ n \times H^+ = n \times H^+_-, \end{cases} \tag{19}$$

- that the magnetic field satisfies the relation (17) in the sheet, *i.e.*

$$n \times H^+_- - n \times H^-_+ = Y_s\, n \times \left(n \times \frac{E^-_+ + E^+_-}{2} \right). \tag{20}$$

Using these assumptions with the interface terms defined in (4) and $\alpha = 0$, one obtains the new interface terms

$$\begin{cases} (n \times E)^{\text{num}} = n \times \dfrac{\{YE\}}{\{Y\}}, \\ (n \times H)^{\text{num}} = n \times H^- + Y_s\, n \times \left(n \times \dfrac{E^- + E^+}{2} \right). \end{cases} \tag{21}$$

The interface terms corresponding to the element '$+$' are obtained in the same way.

DOI: 10.1002/jnm

3. APPLICATION: SHIELDING EFFECTIVENESS OF AN ENCLOSURE OF HETEROGENEOUS WALLS

Let us consider an enclosure manufactured from composite walls (Figure 3). We suppose that the sheet is a dielectric non conductive medium of relative permittivity $\epsilon = 2$, made from $\tau_i = 19.63\%$ of cylindrical conductive fibers (Figure 4). The fibers are of radius $r_i = 0.05mm$, conductivity $\sigma_i = 10^3 S/m$ and relative permittivity $\epsilon_i = 1$. The relative permeabilities are $\mu = \mu_i = 1$.

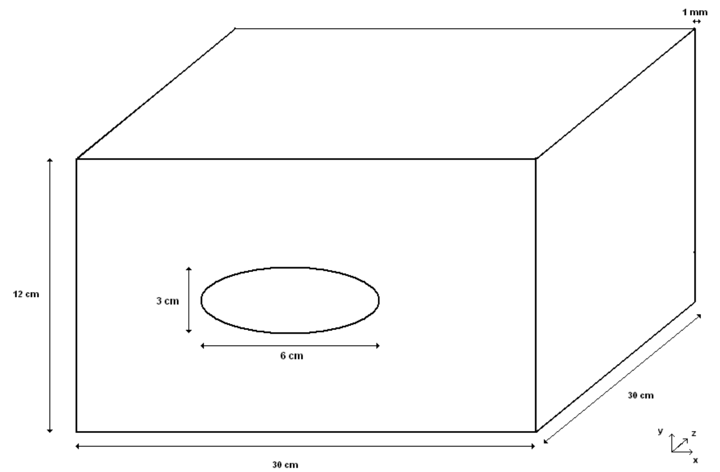

Figure 3. Enclosure of dimension $30cm \times 30cm \times 12cm$ with an elliptically shaped aperture of dimension $10cm \times 0.5cm$.

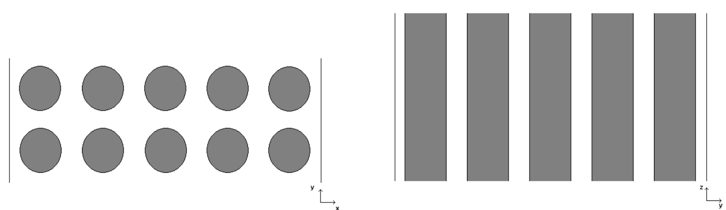

(a) xy (b) yz

Figure 4. Different views of the composite sheet used to manufacture the enclosure.

3.1. *Effective parameters of enclosure walls*

Avoiding to mesh the composite enclosure walls is a crucial issue for modeling this kind of problem. In the frequency domain, the Maxwell-Garnett homogenization approach is a widely used technique for determining the effective parameters for an equivalent homogeneous medium [2] [8]. To check its validity in temporal formulation, the shielding effectiveness of a fully-meshed composite wall is compared to that obtained from homogenized effective parameters. The transverse magnetic (TM) and transverse electric (TE) configurations are considered. Comparisons are performed on the 2D most relevant case presented in Figure 4a.

Periodic boundary conditions are imposed on both the top and bottom borders of the configuration presented in Figure 5. These conditions are equivalent to a magnetic wall for the TE case and to an electric wall for the TM case. A Silver-Muller boundary condition is prescribed at both left and right

Int. J. Numer. Model. (0000)
DOI: 10.1002/jnm

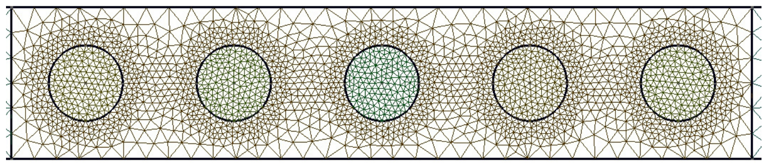

Figure 5. Enclosure

sides of the domain. An incident field is forced through Silver-Muller condition on the right side. This incident field is a transient gaussian pulse of amplitude E of type:

$$E_{inc} = E e^{-(x-ct)^2/D^2}, \tag{22}$$

where D is the spatial width that determines the frequency range.

The transmitted fields are recorded behind the heterogeneous wall and their Fourier transforms are computed. The shielding effectiveness is evaluated using the expression

$$E_{dB} = 20 \log \left| \frac{E_i}{E_t} \right|. \tag{23}$$

3.1.1. Transverse magnetic case The incident fields are defined such as $\vec{E}_i = E_{inc}\hat{z}$ and $\vec{H}_i = -\sqrt{\epsilon_0/\mu_0}\, E_{inc}\hat{y}$. We consider a wall of thickness $e = 1mm$ and 5 conductive fibers of radius $r_i = 0.05mm$. In Figure 6, the Fourier transform of the used incident field and the scattered field are presented.

An equivalent homogeneous conductive sheet is considered. Its effective parameters are constant and depend on the volume ratio of fibers in the wall [14]: $\sigma_{eff} = 0.1963\, \sigma_i = 196\, S/m$ and $\epsilon_{eff} = 0.8037\, \epsilon + 0.1963\, \epsilon_i = 1.8$. The computed shielding effectiveness is compared to the one obtained from an analytical formula in Figure 7. The two results are close. This comparison shows that an equivalent homogenized wall is obtained with only a periodic structure of 5 fibers.

Figure 6. TM case. Fourier transforms of the incident and transmitted electric field.

3.1.2. Transverse electric case The electric and magnetic incident fields are defined such as $\vec{E}_i = E_{inc}\hat{y}$ and $\vec{H}_i = \sqrt{\epsilon_0/\mu_0} E_{inc}\hat{z}$. We consider a wall of thickness $e = 6mm$ and 30 conductive fibers of radius $r_i = 0.05mm$, because the results with $e = 1mm$ thickness are not relevant. In

DOI: 10.1002/jnm

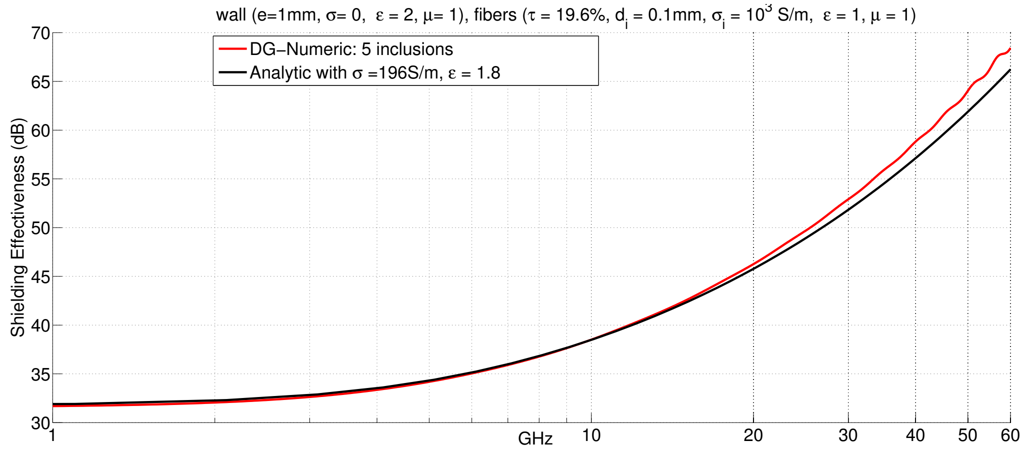

Figure 7. TM case. Comparison of the shielding effectiveness of the composite wall and its homogeneous equivalent with parameters $\sigma_{eff} = 196S/m$ and $\epsilon_{eff} = 1.8$.

Figure 8, the Fourier transform of the used incident field and the transmitted field are presented. The computed shielding effectiveness is compared to that obtained from the Maxwell-Garnett model in Figure 9. Note that the effective parameters are complex-valued and depend on the frequency [7][15]. The two results are similar for frequencies lower than $10GHz$. They differ more and more when the frequency increases. This comparison shows that the Maxwell-Garnett approach is not sufficient to describe an equivalent homogenized wall.

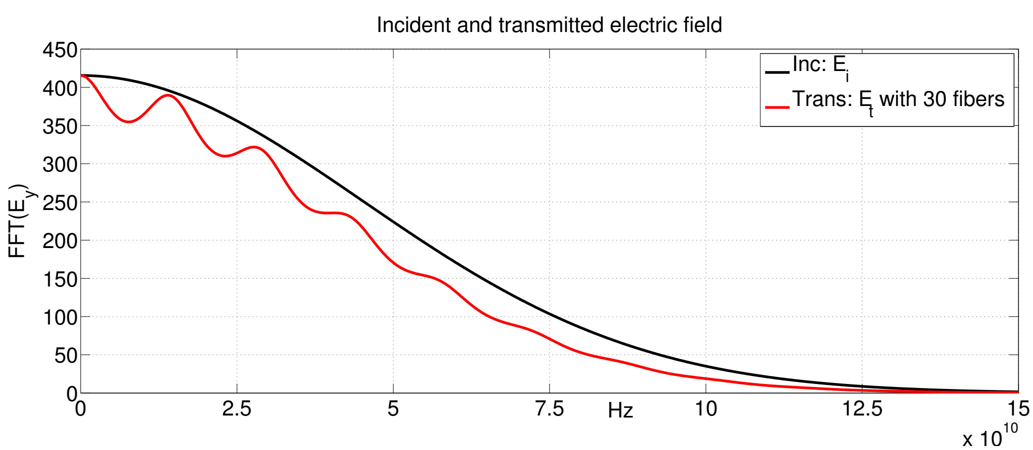

Figure 8. TE case. Incident and transmitted electric field in the frequency domain.

3.2. *Shielding effectiveness of enclosure*

The previous numerical investigations allow us to consider the heterogeneous walls as homogeneous for frequencies lower than $10GHz$. The TM configuration of high shielding effectiveness values is now explored. In this case, the effective parameters obtained from Maxwell-Garnett are: $\sigma_{eff} = 196S/m$, $\epsilon_{eff} = 1.8$ and $\mu_{eff} = 1$. In this frequency range, the skin depth δ of the homogeneous sheet is larger than its thickness. The flux interface for conducting sheets (see 2.2) is used to replace the heterogeneous walls. The simulations are performed on a 3D geometry in the time domain. The number of element is 25774 element. A computer with 32 CPU (2 GHz Pentium Xeon) is used and the CPU time is 15 hours. The incident field is a transient gaussian pulse whose excites

DOI: 10.1002/jnm

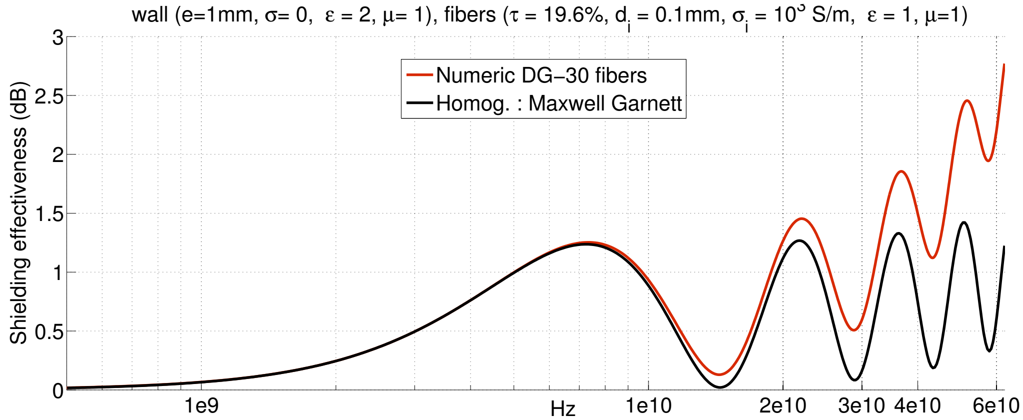

Figure 9. TE case. Comparison of the shielding effectiveness of the composite wall and its homogeneous equivalent with parameters obtained with Maxwell-Garnett model.

frequencies up to 1 GHz. The scattered electric field is recorded at the center of the cavity and presented in Figure 10. The shielding effectiveness is computed for both perfectly and non perfectly conductive walls and is compared to a reference result [13] in Figure 11. The resonance frequency is reproduced. This comparison shows a good consistency of the results obtained from the conducting sheet interface condition.

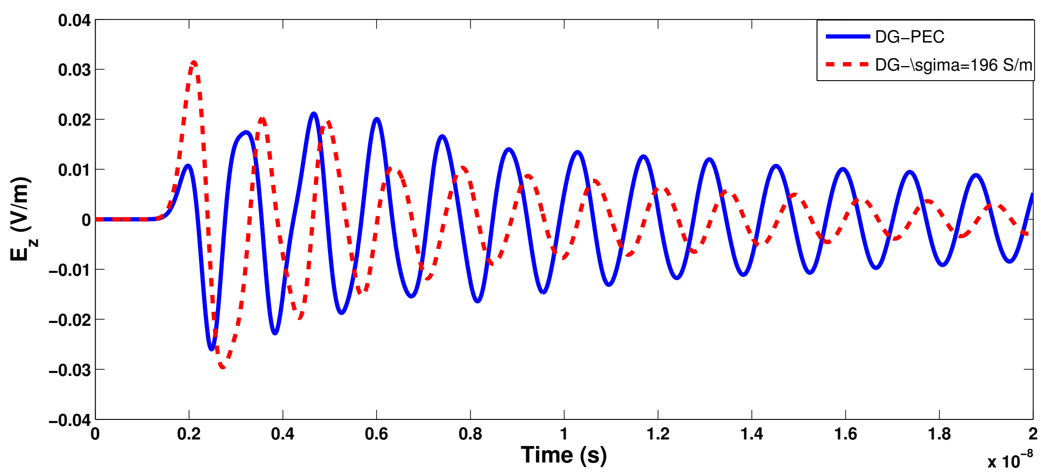

Figure 10. 3D benchmark. Scattering electric field at the center of the enclosure

4. CONCLUSION

This paper presented an analysis of the shielding effectiveness of composite enclosures by using a time domain Discontinuous Galerkin Method. The validity of Maxwell-Garnett homogenization results was studied in the time domain, with gaussian pulses as incident fields. A specific interface condition was proposed to avoid meshing the thin homogeneous conductive walls, allowing to considerably reduce the computational cost of numerical investigations of the composite enclosure.

DOI: 10.1002/jnm

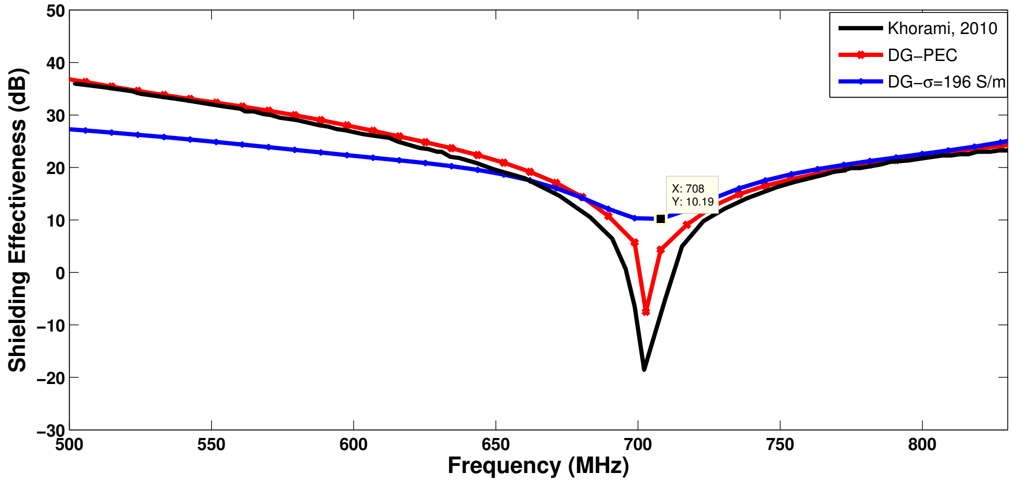

Figure 11. 3D benchmark. Shielding effectiveness of the enclosure evaluated at the center

REFERENCES

1. Holloway CL, Sarto MS, Johansson M. Analyzing Carbon-Fiber Composite Materials with Equivalent-Layer Models . *IEEE transactions on Electromagnetic compatibility* 2005; **47**(4):833-844
2. Koledintseva MY, Dehkhoda P, Mazandaran RM. Modeling of Shielding Composite Materials and Structures for Microwaves frequencies. *Progress In Electromagnetics Research B* 2009; **15**:197-215
3. Araneo R, Lovat G. Fast MoM Analysis of the Shielding Effectiveness of Rectangular Enclosures With Apertures, Metal Plates, and Conducting Objects. *IEEE Trans. Elect. Comp.* 2009; **51**:274-283
4. Wallyn W, De Zutter D, Rogier H. Prediction of The Shielding and Resonant Behavior of Multisection Enclosures Based on Magnetic Current Modeling. *IEEE Trans. Elect. Comp.* 2002; **44**:130-138
5. Kameni A, Modave A, Boubekeur M, Preault V, Pichon L. Evaluation of Shielding Effectiveness of Composite Wall with a Time Domain Discontinuous Galerkin Method. *The European Physical Journal - Applied Physics*. (to appear)
6. Hesthaven JS, Warburton T. Nodal High-Order Methods on Unstructured Grids. *Journal of Computational Physics* 2002; **181**:186-221.
7. Kettunen H, Qi J, Wallén H, Sihvola A. Homogenization of Thin Dielectric Composite Slab: Techniques and Limitations. *ACES Journal* 2011; **26**(4):179-187
8. Qi J, Kettunen H, Wallén H, Sihvola A. Quasi-Dynamic Homogenization of Geometrically Simple Dielectric Composites *ACES Journal* 2010; **25**(12):1036-1045
9. Cockburn B, Hou S, Shu CW. The Runge-Kutta Local Projection Discontinuous Galerkin Finite Element Method for Conservation Laws IV: The Multidimensional Case. *Math Comp* 1990; **54**:454-581.
10. Cockburn B, Li F, Shu CW. Locally divergence-free discontinuous Galerkin methods for the Maxwell equations. *J. Comp. Phys*2004; **194**:588-610.
11. Lu T, Zhang P, Cai W. Discontinuous Galerkin methods for dispersive and lossy Maxwell's equations and PML boundary conditions. *J. Comp. Phys*2004; **200**:549-580.
12. Fezoui L, Lanteri S, Lohrengel S, Piperno S. Convergence and Stability of a Discontinuous Galerkin Time-Domain Method for the 3D Heterogeneous Maxwell Equations on Unstructured Meshes.*M2AN* 2005; **39**(6):1149-1176.
13. Khorami MA, Dehkhoda P, Mazandaran RM. Fast Shielding Effectiveness Calculation of Metallic Enclosures With Apertures Using a Multiresolution Method of Moments Technique. *IEEE Trans. Elect. Comp.* 2010; **52**:230-235
14. Gaier JR. Intercalated graphite fiber composites as EMI in aerospace structures *IEEE Trans Electromagnetic Comp* 1992;**34**(3):351-356.
15. Mori T, Tanaka R. Average Stress in Matrix and Average Elastic Energy of Materials With Misfitting Inclusions . *Acta Metall Mater* 1973; **21**:597-629.

Int. J. Numer. Model. (0000)
DOI: 10.1002/jnm